Bol. Soc. Esp. Mat. Apl.
n^{o}47(2009), 73–80

MULTIRESOLUTION SIMULATION OF REACTION-DIFFUSION SYSTEMS WITH STRONG DEGENERACY

RAIMUND BÜRGER[†], RICARDO RUIZ-BAIER[‡]

[†]CI^{2}MA and Departamento de Ingeniería Matemática,
Universidad de Concepción, Casilla 160-C, Concepción, Chile
[‡]IACS, Chair of Modelling and Scientific Computing, École Polytechnique Fédérale de Lausanne,
Station 8, CH-1015, Lausanne, Switzerland

rburger@ing-mat.udec.cl, ricardo.ruiz@epfl.ch

Abstract

A fully space-adaptive multiresolution method is applied to an explicit finite volume scheme for solving a strongly degenerate reaction-diffusion system. Since a closed mathematical theory is lacking, insight into the behaviour of these systems, in particular into the spatial patterns their solutions may exhibit, can be currently obtained by numerical experimentation only. It is demonstrated that the present space-adaptive scheme is an appropriate tool for this purpose. In particular, the multiresolution method and the classical finite volume scheme are compared and the numerical results show that this strategy provides substantial savings in terms of data storage and computational effort, while giving an accurate approximation to the sought quantities.

Key words: *Adaptive multiresolution schemes, Degenerate diffusion, Pattern-formation, Turing instability.*

AMS subject classifications: *65M06, 35K55.*

1 Introduction

In [1] we present a fully adaptive multiresolution (MR) scheme for spatially 2D, possibly degenerate reaction-diffusion systems, focusing on models of combustion, pattern formation, and chemotaxis. Solutions of these equations in these applications often exhibit steep gradients, and in the degenerate case, sharp fronts and discontinuities. This calls for a concentration of computational effort to zones of strong variation.

In this note we investigate the influence of the form of the diffusion terms, constructed so that the governing equations form a strongly degenerate parabolic system, on the spatial patterns shown by the system. To consider *degenerate* diffusion as a mechanism for the creation of Turing-like instabilities seems to be a novelty in the context of two-dimensional reaction-diffusion systems. The proposed MR scheme is based on finite volume discretizations with explicit time stepping, and the efficiency of the method relies in part on the strategy for storing the solution, namely a dynamic graded tree, whose leaves are the non-uniform finite volumes on the borders of which the numerical divergence is evaluated. By a thresholding procedure, which accounts for the elimination of leaves that are smaller than a threshold value, substantial data compression and CPU time reduction is attained.

We specifically consider the reaction-diffusion system

$$u_t = \gamma f(u,v) + \Delta A(u) \quad \text{on } Q_T := \Omega \times (0,T),\ \Omega := (0,1)^2, \tag{1a}$$

$$v_t = \gamma g(u,v) + d\Delta B(v) \quad \text{on } Q_T, \tag{1b}$$

$$u(x,0) = u_0(x), \quad v(x,0) = v_0(x) \quad \text{for } x \in \Omega, \tag{1c}$$

$$\nabla A(u) \cdot \mathbf{n} = \nabla B(u) \cdot \mathbf{n} = 0 \quad \text{on } \Sigma_T := \partial\Omega \times (0,T). \tag{1d}$$

This system models several phenomena including combustion and chemotaxis [1], but is considered here as the generalization of a well-known model of pattern formation in mathematical biology [6]. Under a number of structural conditions relating the functions $f(u,v)$ and $g(u,v)$ and their derivatives to the parameters γ and d, the system (1) with $A(u) = B(u) = u$ produces stationary solutions with Turing-type spatial patterns [6]. To produce this effect, we could select these diffusion terms along with the kinetics $f(u,v) = a-u+u^2v$ and $g(u,v) = b-u^2v$, with the parameters $a = -0.5$, $b = 1.9$, $d = 4.8$, and $\gamma = 210$ [6]. In this work, however, the diffusion terms are chosen to be strongly degenerate:

$$A(u) = \begin{cases} 0 & \text{for } u \leqslant u_\mathrm{c}, \\ u - u_\mathrm{c} & \text{otherwise} \end{cases}, \quad B(u) = \begin{cases} 0 & \text{for } u \leqslant v_\mathrm{c}, \\ u - v_\mathrm{c} & \text{otherwise,} \end{cases} \quad u_\mathrm{c}, v_\mathrm{c} \geqslant 0. \tag{2}$$

It turns out that even if the stability analysis performed in [6] does *not* apply to the strongly degenerate case, our numerical experiments in Section 4 lead to the formation of spatial patterns. Holden et al. [5] prove existence and uniqueness of entropy solutions of weakly coupled systems of degenerate parabolic equations in an unbounded domain; the well-posedness analysis for (1) is, however, still an open problem due to the boundary condition (1d), which is not covered by the analysis of [5]. Turing instabilities driven by other non-standard diffusion terms, namely by fractional diffusion, have been studied e.g. by Nec and Nepomnyashchy [7].

The remainder of the paper is organized as follows. Section 2 contains a description of the construction of the reference FV formulation used to numerically solve the underlying problem. In Section 3 we detail the main ingredients of the MR framework needed to provide space adaptivity to the overall numerical scheme, and the numerical results provided in Section 4 confirm that the adaptive MR method provides high rates of data compression and CPU time speed-up, while the error remains controlled.

2 Finite volume discretization

An admissible mesh for Ω is formed by a family $\mathcal{T}$ of control volumes (open and convex polygons) of maximum diameter h. For all $K \in \mathcal{T}$, x_K denotes the center of K, $N(K)$ the set of neighbors of K, $\mathcal{E}_{\text{int}}(K)$ is the set of edges of K in the interior of $\mathcal{T}$ and $\mathcal{E}_{\text{ext}}(K)$ the set of edges of K on the boundary $\partial\Omega$. For all $L \in N(K)$ $d(K,L)$ denotes the distance between x_K and x_L, $\sigma_{K,L}$ is the interface between K and L and $\eta_{K,L}$ ($\eta_{K,\sigma}$ respectively) is the unit normal vector to $\sigma_{K,L}$ ($\sigma \in \mathcal{E}_{\text{ext}}(K)$ respectively) oriented from K to L (from K to $\partial\Omega$ respectively). For all $K \in \mathcal{T}$, $|K|$ stands for the measure of the cell K. From the admissibility of $\mathcal{T}$ we have that $\overline{\Omega} = \cup_{K\in\mathcal{T}}\overline{K}$, $K \cap L = \varnothing$ if $K, L \in \mathcal{T}$ and $K \neq L$, and there exists a finite sequence $(x_K)_{K\in\mathcal{T}}$ for which $\overline{x_K x_L}$ is orthogonal to $\sigma_{K,L}$. Now, consider $K \in \mathcal{T}$ and $L \in N(K)$ with common vertices $(a_{\ell,K,L})_{1\leqslant\ell\leqslant I}$ with $I \in \mathbb{N}\backslash\{0\}$ and let $T_{K,L}$ (respectively $T^{\text{ext}}_{K,\sigma}$ for $\sigma \in \mathcal{E}_{\text{ext}}(K)$) be the open and convex polygon with vertices (x_K, x_L) (x_K respectively) and $(a_{\ell,K,L})_{1\leqslant\ell\leqslant I}$. For all $K \in \mathcal{T}$, the approximation $\nabla_h u_h$ of ∇u is defined by

$$\nabla^h_L u_h(x) = \begin{cases} |T_{K,L}|^{-1}|\sigma_{K,L}|(u_L - u_K)\eta_{K,L} & \text{if } x \in T_{K,L}, \\ 0 & \text{if } x \in T^{\text{ext}}_{K,\sigma}. \end{cases}$$

Now we choose an admissible mesh for Ω and a time step size $\Delta t > 0$. We may choose $N > 0$ as the smallest integer such that $N\Delta t \geqslant T$, and set $t^n := n\Delta t$ for $n \in \{0, \dots, N\}$. The discretized reaction terms are defined as $f^{n+1}_K := f(u^{n+1}_K, v^{n+1}_K)$ and $g^{n+1}_K = g(u^{n+1}_K, v^{n+1}_K)$ and the nonlinear diffusions are constructed using the terms $A^{n+1}_K := A(u^{n+1}_K)$ and $B^{n+1}_K := A(v^{n+1}_K)$. Incorporating an explicit first order Euler time integration, the resulting FV scheme reads: Determine $(u^{n+1}_K)_{K\in\mathcal{T}}$, $(v^{n+1}_K)_{K\in\mathcal{T}}$ such that

$$\frac{u^{n+1}_K - u^n_K}{\Delta t} + \sum_{L\in N(K)} \nabla^h_L A^n_K = f^n_K, \quad \frac{v^{n+1}_K - v^n_K}{\Delta t} + \sum_{L\in N(K)} d\nabla^h_L B^n_K = g^n_K, \quad (3)$$

for all $K \in \mathcal{T}$. The boundary condition is taken into account by imposing zero fluxes on external edges. The resulting finite volume scheme has a unique solution that converges to the weak solution of (1) in the non-degenerate case [4]. Moreover, according to [5] this scheme is stable under the CFL condition

$$h^{-1}\Delta t\gamma \max_{K\in\mathcal{T}}\big(|f^u_K| + |f^v_K| + |g^u_K| + |g^v_K|\big) + 4h^{-2}\Delta t \max_{K\in\mathcal{T}}\big(|A'_K| + d|B'_K|\big) \leqslant 1,$$

where $f^u_K := \partial_u f(u_K, v_K)$ and $A'_K := A'(u_K)$, for $K \in \mathcal{T}$.

3 Multiresolution representation

For further details on the one-dimensional theory, we refer to the fairly complete description in [3]. For ease of computations, we only consider rectangular meshes on a rectangular domain, which after a change of variables can be regarded as $\Omega = [0,1]^2$. Nevertheless, the multiresolution analysis could be carried out for non-structured meshes. Firstly, a nested mesh hierarchy $\mathcal{T}_0 \subset \cdots \subset \mathcal{T}_L$ using a partition of Ω is constructed, where each grid $\mathcal{T}_l$ is formed by the control volumes on each level K^l, $l = 0, \dots, L$. Here $l = 0$ corresponds to the coarsest and $l = L$ to the finest resolution level and the so called *refinement sets* are defined by $M_{K,l} = \{L_i^{l+1}\}_i$ and $\overline{K^l} = \cup_{i=1}^{\# M_{K,l}} L_i^{l+1}$. For $x \in K^l$ the *scale box function* is defined as $\tilde{\varphi}_{K,l}(x) := |K^l|^{-1}\chi_{K^l}(x)$ and the average of any function $u(\cdot,t) \in L^1(\Omega)$ in the cell K^l may be written as $u_{K,l} := \langle u, \tilde{\varphi}_{K,l}\rangle_{L^1(\Omega)}$.

It is known that cell averages and box functions satisfy the two-level relation

$$\tilde{\varphi}_{K,l} = \sum_{L_i^{l+1} \in M_{K,l}} \frac{|L_i^{l+1}|}{|K^l|} \tilde{\varphi}_{L_i,l+1}, \quad \bar{u}_{K,l} = \sum_{L_i^{l+1} \in M_{K,l}} \frac{|L_i^{l+1}|}{|K^l|} u_{L_i,l+1}, \tag{4}$$

which defines a *projection* operator needed to move from finer to coarser levels. For $x \in K^{l+1}$ the *wavelet function* is defined by

$$\tilde{\psi}_{K,j,l} = \sum_{L_i^{l+1} \in M_{K,l}} \frac{|L_i^{l+1}|}{|K^l|} (-1)^{ij} \tilde{\varphi}_{L_i,l+1} \quad \text{for } j = 1, \dots, \# M_{K,l},$$

and from (4), a similar inverse two-level relation holds. *Detail coefficients* are defined as $d_{K,j,l} := \langle u, \tilde{\psi}_{K,j,l}\rangle$ for $j = 1, \dots, \# M_{K,l}$. An appealing feature is that a transformation between the cell averages on level L and the cell averages on level zero plus a series of details can be determined and such transformation should be reversible. Therefore

$$\tilde{u}_{K,l+1} = \sum_{T \in \bar{S}_K^l} g_{K,T}^l u_{T,l}, \tag{5}$$

where $\bar{S}_K^l$ is the stencil of interpolation or *coarsening set*, $g_{K,T}^l$ are coefficients, and the tilde over u in the left-hand side of (5) denotes a predicted value. In this way, a *prediction* operator is defined, which is imposed to be local and consistent with the projection and will be necessary to move from coarser to finer resolution levels. For rectangular meshes it corresponds to $\tilde{u}_{L_i,l+1} = u_{L,l} - Q_x - Q_y + Q_{xy}$ for $i = 1, \dots, \# M_{K,l}$, where

$$Q_z := \sum_{n=1}^{s} \tilde{\gamma}_n \big(u_{S_z,l} - u_{T_z,l}\big), \quad z \in \{x, y\},$$
$$Q_{xy} := \sum_{n=1}^{s} \tilde{\gamma}_n \sum_{p=1}^{s} \tilde{\gamma}_p \big(u_{S_{x,y},l} - u_{S_{x,-y},l} - u_{S_{-x,y},l} + u_{S_{-x,-y},l}\big).$$

Here $S_{\pm x, \pm y}$ denote the neighbors of the corner of the control volume S and the corresponding coefficients are $\tilde{\gamma}_1 = -\frac{22}{128}$ and $\tilde{\gamma}_2 = \frac{3}{128}$ (see [8]). Details are related to the regularity of a given function. The more regular u is over K^l, the smaller is the corresponding detail coefficient. Therefore a *thresholding* procedure is also applied, which basically consists in discarding all control volumes corresponding to details that are smaller in absolute value than a level-dependent tolerance. Denoting by α the experimental convergence rate of (3) and by ε_{R} given a reference tolerance determined by (see e.g. [1, 2] for details)

$$\varepsilon_{\mathrm{R}} = \frac{C 2^{-(\alpha+2)L}}{|\Omega| \max_{K \in \mathcal{T}} \left(|f_K^u| + |f_K^v| + |g_K^u| + |g_K^v|\right) + |\Omega|^{3/2} 2^{L+2} \max_{K \in \mathcal{T}} \left(|A_K'| + d|B_K'|\right)},$$

we obtain level-dependent tolerances ε_l defined by $\varepsilon_l = 2^{2(l-L)}\varepsilon_{\mathrm{R}}$, $l = 0, \dots, L$. We organize the cell averages and corresponding details at different levels in a *dynamic graded tree*. The *root* is the basis of the tree, a parent node has four sons, and the sons of the same parent are called *brothers*. A node without sons is a *leaf* and a given node has $s' = 2$ *nearest neighbors* in each spatial direction, needed for the computation of the fluxes of leaves; if these neighbors do not exist, we create them as *virtual leaves*. We denote by Λ the set of all nodes of the tree and by $\mathcal{L}(\Lambda)$ the set of leaves. We apply this MR representation to the spatial part of the pair $\mathbf{u} = (u, v)$, which corresponds to the numerical solution of the underlying problem for each time step, so we need to update the tree structure for the proper representation of the solution during the evolution. To this end, we apply a thresholding strategy, but always keep the graded tree structure of the data. Once the thresholding is performed, we add to the tree a *safety zone*, generated by adding one finer level to the tree in all leaves without violating the graded tree data structure.

The *data compression rate* $\eta := N/(2^{-(2L)}N + \#\mathcal{L}(\Lambda))$ and *speed-up rate* $\mathcal{V} := \text{CPU time}_{\text{FV}}/\text{CPU time}_{\text{MR}}$ are used to measure the improvement in data and CPU time compression respectively. Here, N is the number of control volumes in the full finest grid at level L, and $\#\mathcal{L}(\Lambda)$ is the number of leaves.

4 Numerical experiments

As a first numerical result, we consider a computation starting from a random perturbation of the steady state ($u_0 = a + b = 1.4, v_0 = b/(a+b)2 = 0.96939$) and we use $L = 9$ resolution levels and a reference tolerance given by $\varepsilon_{\mathrm{R}} = 7.82 \times 10^{-4}$. The computational domain is the unit square $\Omega = [0,1]^2$. Figure 1 presents the numerical solution for non-degenerate diffusion, i.e., we choose $A(u) = B(u) = u$. (See [1] for further examples of this case).

Being one of our main interests studying the effect of degenerate diffusion, we present in Example 2 several cases in which all parameters remain the same, except for the test parameters which are the critical concentrations $u_{\mathrm{c}}, v_{\mathrm{c}}$ used in (2). Those cases are $u_{\mathrm{c}} = u_0 + c$, $v_{\mathrm{c}} = v_0 + c$, with $c \in \{0, 0.5, 2.0\}$. In Figure 2 we display the component v of the numerical solution and the leaves of the corresponding tree structure at a transient state at time $t = 1.5$ for all test cases and it is clear that the larger the value of c, the more chaotic the spatial patterns shown by the corresponding system. This behaviour could be explained by the increasing incoherence between solution values at different points.

For Example 3, we select one of the cases from the previous example and perform a study of the error. The effectiveness of the MR method is illustrated

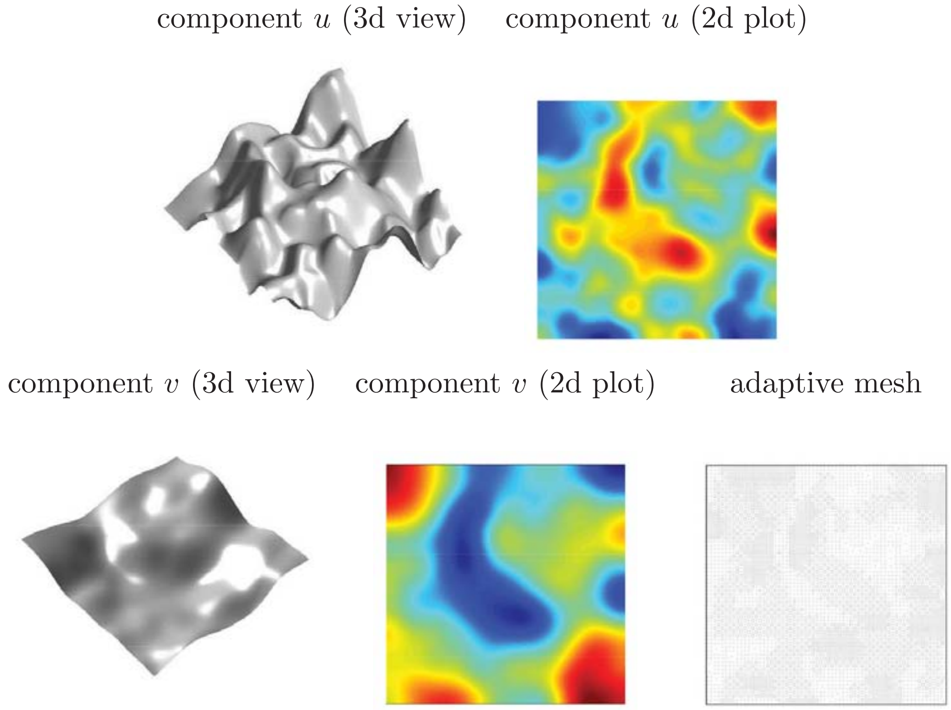

Figure 1: *Example 1: Component* v *and corresponding adaptive mesh at* $t = 1.5$ *for non-degenerate diffusion. The solution assumes values* $1.390 < u < 1.402$ *and* $0.96988 < v < 0.96998$.

in Table 1, specifically displaying the corresponding simulated time, speedup $\mathcal{V}$, data compression rate η, and normalized errors in different norms for both components of the solution. These errors are obtained by comparing with an approximate solution given by a reference FV computation on a fine mesh of 4194304 control volumes. In addition, from Figure 3 a experimental rate of convergence of about 1.9 is noticed for the adaptive MR scheme. As seen in [1], a slightly better rate of convergence may be also obtained by the MR method for the non-degenerate problem.

Acknowledgements

RB acknowledges support by Fondecyt (Chile), project 1090456, Fondap in Applied Mathematics (project 15000001), and BASAL project CMM, Universidad de Chile and Centro de Investigación en Ingeniería Matemática (CI^{2}MA), Universidad de Concepción.

References

[1] M. Bendahmane, R. Bürger, R. Ruiz-Baier, K. Schneider, *Adaptive multiresolution schemes with local time stepping for two-dimensional degenerate reaction-diffusion systems*, Appl. Numer. Math., to appear.

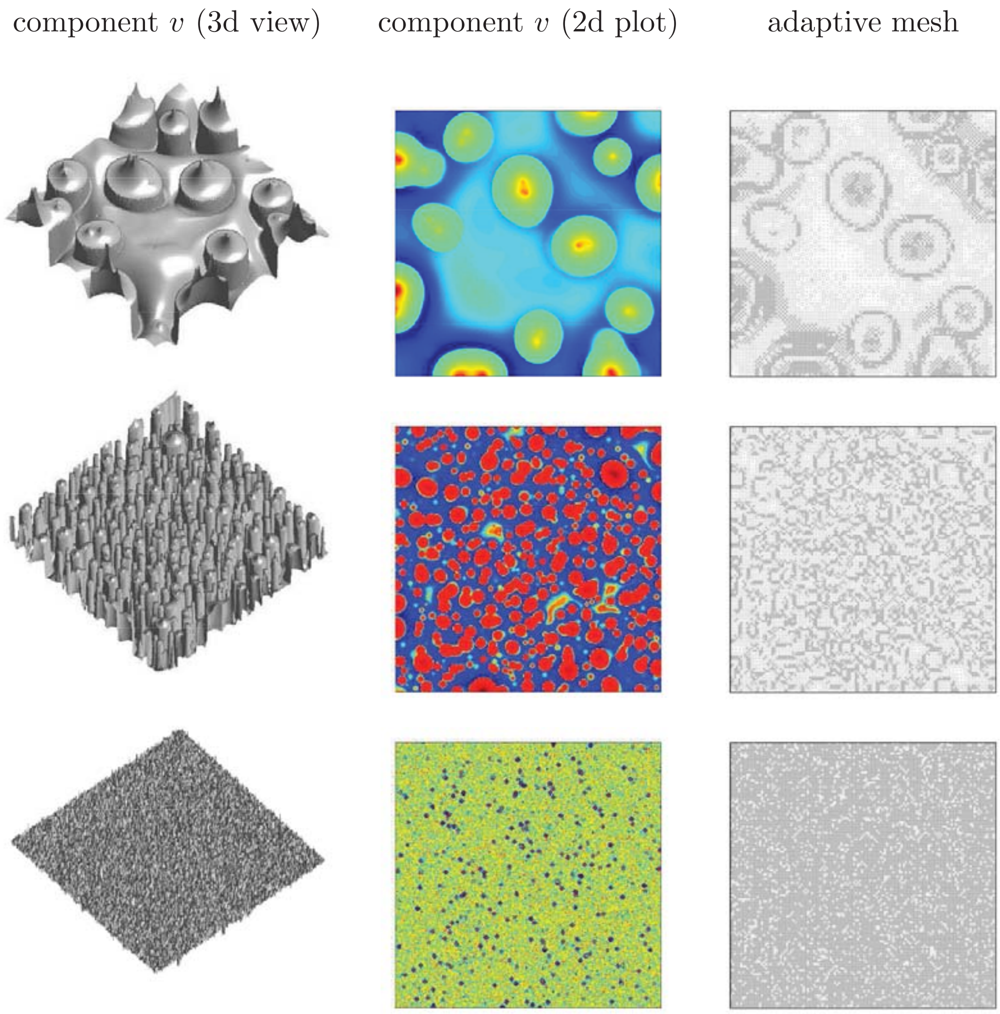

Figure 2: *Example 2: Component v and corresponding adaptive mesh at $t = 1.5$ for $c = 0$ (top), $c = 0.5$ (middle) and $c = 2.0$ (bottom). The solution assumes values $0.96 < v < 0.98$, $0.96 < v < 0.99$ and $0.84 < v < 1.08$ respectively.*

t	$\mathcal{V}$	η	Species	L^1-error	L^2-error	$L^\infty-$error
0.05	9.41	12.7219	u	3.52×10^{-4}	3.65×10^{-4}	6.34×10^{-4}
			v	2.70×10^{-4}	3.08×10^{-4}	5.22×10^{-4}
0.5	12.27	17.9721	u	5.19×10^{-4}	6.13×10^{-4}	6.57×10^{-4}
			v	4.82×10^{-4}	7.06×10^{-4}	1.18×10^{-3}
1.5	12.93	18.7118	u	5.23×10^{-4}	6.65×10^{-4}	9.47×10^{-4}
			v	5.90×10^{-4}	8.31×10^{-4}	2.04×10^{-3}

Table 1: *Example 3: Model with $c = 0$. Corresponding simulated time, speedup $\mathcal{V}$, data compression rate η and errors in different norms.*

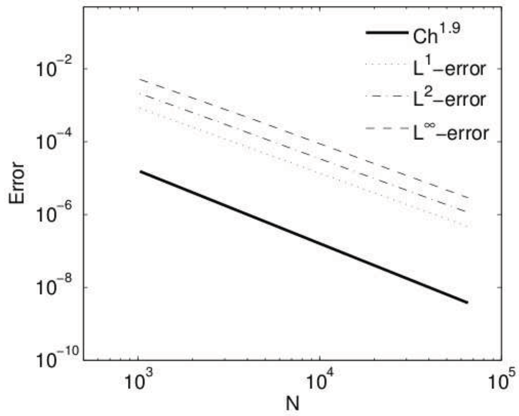

Figure 3: *Example 3: Turing model for* $c = 0$*. Errors in different norms for the MR method at* $t = 1.5$*.*

[2] R. Bürger, R. Ruiz-Baier, K. Schneider, M. Sepúlveda, *Fully adaptive multiresolution schemes for strongly degenerate parabolic equations in one space dimension*, M2AN Math. Model. Numer. Anal. 42 (2008) 535–563.

[3] A. Cohen, S. Kaber, S. Müller, M. Postel, *Fully adaptive multiresolution finite volume schemes for conservation laws*, Math. Comp. 72 (2003) 183–225.

[4] R. Eymard, Th. Gallouët, R. Herbin, *Finite Volume Methods*. In: P.G. Ciarlet, J.L. Lions (eds.), Handbook of Numerical Analysis, vol. VII, North-Holland, Amsterdam, (2000) 713–1020.

[5] H. Holden, K.H. Karlsen, N.H. Risebro, *On uniqueness and existence of entropy solutions of weakly coupled systems of nonlinear degenerate parabolic equations*, Electron. J. Differential Equations 46 (2003), pp. 1–31.

[6] J.D. Murray, *Mathematical Biology II: Spatial Models and Biomedical Applications*, Third Edition, Springer-Verlag, New York (2003).

[7] Y. Nec, A.A. Nepomnyashchy, *Turing instability of anomalous reaction-anomalous diffusion systems*, Eur. J. Appl. Math. 19 (2008), pp. 329–349.

[8] O. Roussel, K. Schneider, A. Tsigulin, H. Bockhorn, *A conservative fully adaptive multiresolution algorithm for parabolic PDEs*, J. Comput. Phys. 188 (2003) 493–523.